Performance of an Advanced ATD Thorax System in Frontal Crash Environments

Alena V. Hagedorn — Transportation Research Center, Inc.
East Liberty, Ohio
USA

Mark P. Haffner — National Highway Traffic Safety Administration
U. S. Department of Transportation
Washington, D.C.
USA

Lawrence W. Schneider — University of Michigan
Transportation Research Institute
Ann Arbor, Michigan
USA

Abstract

This paper describes the results of laboratory evaluation of an advanced ATD thorax system, denoted TAD-50M (Trauma Assessment Device, 50th percentile male), which has been integrated with Hybrid III lower and upper extremity, neck, and head components for testing. Tbe evaluation program consisted of pendulum, quasi-static thorax compression, and sled tests in a variety of restraint environments, including air bag, two-point belt/knee bolster, and three-point belt systems. TAD-50M thorax instrumentation included four internal thoracic displacement measurement assemblies. Two externally mounted chest bands were also utilized during sled tests. Baseline sled tests utilizing the Hybrid III ATD were also conducted and are reported.

Introduction

This test program represents the first extensive performance evaluation of the TAD-50M design. The test protocol was designed to evaluate overall prototype performance in a wide variety of restraint environments, and to assess durability and biofidelity of the new design.

The broad goal of the TAD-50M thorax system development effort was the design of an ATD thorax assembly with enhanced capability to assess thoracic injury potential to vehicle occupants restrained by belts and air bags. A specific goal was the development of a thoracic test device that could reliably assess performance of combined belt/ air bag restraint systems.

These goals were approached in the thorax design by incorporating realistic thoracic and spinal anthropometry, more humanlike coupling between thoracic regions, improved regional impact response biofidelity, and more comprehensive chest deflection instrumentation.

Description of Prototype

The TAD-50M thorax system (hereafter referred to as the "TAD") is shown in Figures 1 and 2 is described in detail in (1)[1]. Therefore, only a brief overview of the design is provided in this paper.

To accomplish the stated goals, the design includes the following general features:

- realistic vehicle-seated posture and anthropometry, including representation of upper and lower ribcage geometry important to torso belt interaction;
- biofidelic impact response at both the sternum and lower ribcage locations;
- improved regional stiffness and interregional coupling behavior;
- representation of the clavicle to provide humanlike upper belt load path to the chest;
- a new shoulder assembly with more realistic kinematic behavior; and
- introduction of an articulating thoracic spine.

Instrumentation supplied with the prototype includes:

- three-dimensional thoracic displacement measurement assemblies at four sites on the anterior ribcage, bilaterally at the sternum and at lower ribcage locations;
- Y-axis angular velocity/position sensors on the upper and lower thoracic spine segments, in addition to the pelvis, for computation of planar spinal kinematics; and
- a frangible abdominal insert to detect belt or steering wheel rim intrusion.

[1]Reference (1) refers to the TAD-50M as the Prototype-50M

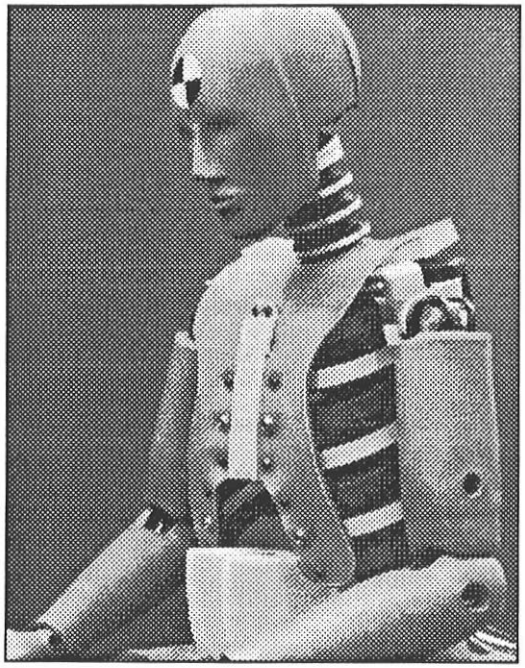

Figure 1. TAD Thorax

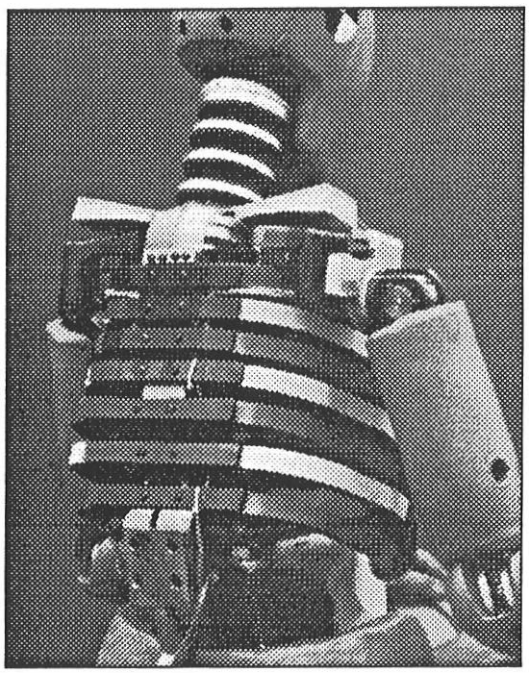

Figure 2. TAD Thorax

A description of additional instrumentation installed in the prototype during testing will be provided below.

Scope of Test Program

Tests conducted to evaluate the performance of the TAD thorax system consisted of 21 quasi-static thoracic compression tests, 37 pendulum tests, and 12 full-scale sled tests. The full sled test series conducted, including baseline Hybrid III tests, is shown in Table 1. The emphasis of the sled test series was to determine the sensitivity of the TAD to various restraint environments as well as to assess the durability of the thorax system design.

TABLE 1. TAD-50M and Hybrid III Sled Test Matrix

	TEST #	DESCRIPTION
TAD-50M Torso:	472-473:	3 pt. belt with air bag frontal test at 48 kph (30 mph) (driver)
	474 :	Air bag only frontal test at 48 kph - no lap belt (driver)
	475-476:	3 pt. belt frontal test at 48 kph (driver)
	477 :	2 pt. belt/knee bolster system frontal test at 48 kph (passenger)
	478 :	Air bag/lap belt frontal test at 48 kph (driver)
	479 :	3 pt. belt with air bag frontal test at 56 kph (35 mph) (driver)
	480 :	Air bag with lap belt frontal test at 56 kph (driver)
	481 :	3 pt. belt frontal test at 56 kph (driver)
	482 :	3 pt. Belt with air bag oblique test at 48 kph (driver)
	483 :	3 pt. belt oblique test at 48 kph (driver)
Hybrid III Stringpot Thorax:	485 :	Air bag with lap belt frontal at 48 kph (driver)
	486 :	3 pt. belt at 48 kph (driver)

The following sections describe and discuss TAD-50M pendulum and sled test results. Hybrid III data are included for reference and general comparison. Quasi-static tests were performed primarily to validate the thoracic deflection instrumentation and the accompanying software, and are not included in this paper. Results of the quasi-static tests revealed the chest displacement instrumentation accuracy to be within approximately 2 mm of measured values.

TAD Deflection Measurement Assemblies

The construction and installation of a typical displacement measurement assembly, called a double-gimballed stringpot (DGSP), is shown schematically in Figure 3. Four such assemblies are installed in the thorax. Two assemblies are attached bilaterally at the sternum, 3.8 cm on each side of the mid-sagittal plane, at the human anatomical equivalent location of rib 4/5 interspace. The other two assemblies are attached bilaterally at the lower ribcage, 8.3 cm on each side of the mid-sagittal plane, at the human anatomical equivalent location of rib 8. (Note that these are not the same as ATD rib numbers; e.g., the TAD prototype has only seven ribs. See Figures 1 and 2.)

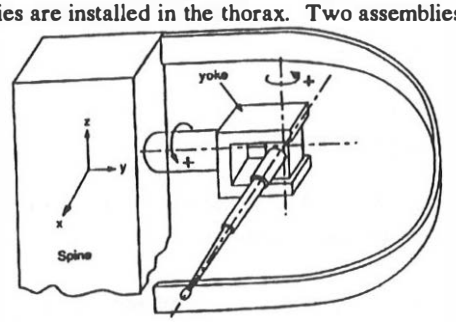

Figure 3. TAD Double Gimballed Stringpot Assembly

Each DGSP assembly consists of a telescoping tubular joy stick connected front to back, with joy stick length continuously monitored by a coaxial string potentiometer. Each telescoping joy stick is mounted to the TAD lower thoracic spine segment via a double gimbal, with potentiometer measurement of rotational displacement of both gimbals. Thus, each DGSP assembly captures three dimensional motion of its anterior attachment point relative to its lower thoracic spine attachment. Dedicated software interprets the stringpot and rotary potentiometer outputs as changes in X, Y, and Z displacement of the anterior attachment point relative to the spinal axis coordinate system.

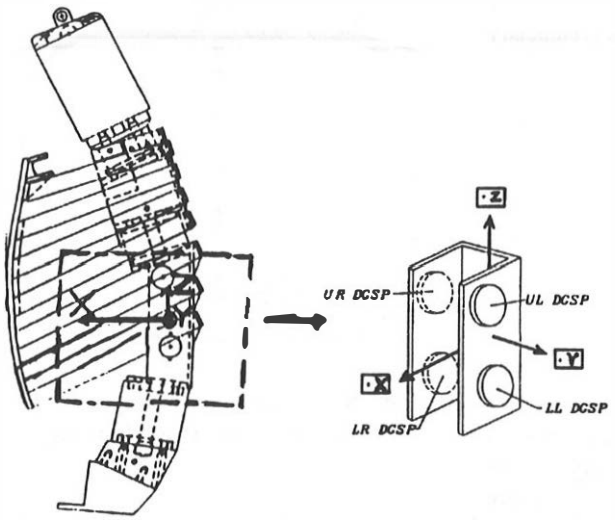

Figure 4. TAD Spinal Axis Coordinate System

The primary reference system for the TAD is the spinal axis coordinate system, shown in Figure 4. This coordinate system has its origin at the lower thoracic spine segment. The positive X-axis, which is perpendicular to the front surface of the lower spine, points forward, positive Y is to the left, and positive Z is upward. The coordinate system follows the right hand rule sign convention for rotations about X, Y, and Z.

Pendulum Tests

The TAD-50M thorax was tested on the pendulum using a 23.2 kg, 152-mm-diameter rigid impactor. An accelerometer mounted to the ram of the impactor mass was used to measure impact force and thereby enable computation of force-deflection curves. Tests were conducted at the level of midsternum for impact velocities of 4.3 m/s and 6.7 m/s and at the lower ribcage for an impact velocity of 4.3 m/s.

For mid sternum pendulum impacts, the TAD thorax is positioned so that the X-axis (Figure 5) is directed horizontally. This places the X-axis for sternal deflection computations coincident with the axis of pendulum-to-thorax impact (the axis of compression), and allows direct comparison of TAD-50M thorax force-deflection data with the Kroell (2,3) pendulum force-deflection corridors.

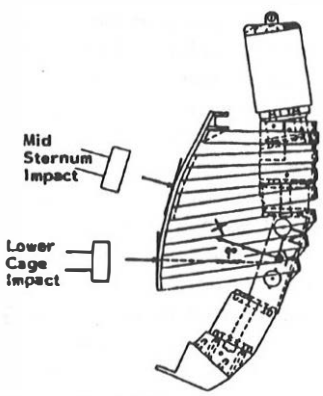

Figure 5. TAD Compression Axes for Pendulum Impact Tests

Figures 6 and 7 show the force deflection response curves for sternal impacts at 4.3 m/s and 6.7 m/s, respectively, where the dashed-line corridors indicate the desired human response corridors developed by Neathery (4) from the Kroell et al. (2,3) data base. Results are shown for the upper right deflection assembly and are calculated along the X- axis of compression which is coincident with the X-axis described previously (Figure 5). Similar deflections were seen for the upper left displacement measurement assembly. At 6.7 m/s the response falls within the recommended corridor. At 4.3 m/s the computed peak inward deflection falls short of the desired corridor.

As indicated in the legends, the two curves in each plot are for tests conducted before and after the series of most pendulum and all sled tests. The good agreement in both cases suggests that the TAD-50M prototype possesses excellent durability. These plots show little shift for tests run before and after the series of 70 tests (37 pendulum

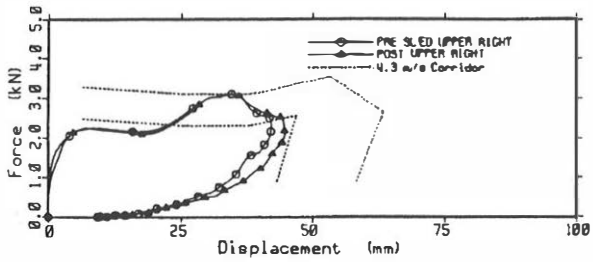

Figure 6. TAD Pre and Post Sled Test Pendulum Impacts - 4.3 m/s Mid Sternum

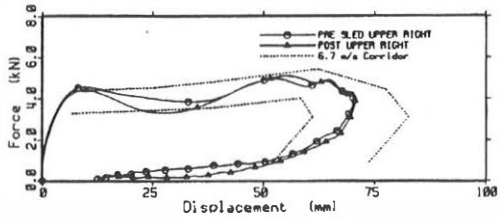

Figure 7. TAD Pre and Post Sled Test Pendulum Impacts - 6.7 m/s Mid Sternum

impact, 21 quasi-static compression, and 12 sled tests) conducted using the torso. The thorax was designed to sustain 50 to 100 impact exposures (5) and the fact that the thorax response did not shift after the test series indicates its ability to meet design goals. In addition, there was no apparent degradation of the rib damping material after the 70 tests, further indicating durability.

Impacts were also performed at the lower left ribcage at 4.3 m/s. At the lower ribcage locations, the impact was directed along a line 9 degrees downward from the X-axis (Figure 5) and 12 degrees outward from the X-axis (Figure 8). Therefore, X-deflections from pendulum impacts to the lower ribcage are calculated along this rotated X-axis of compression for purposes of comparison with the preliminary corridor developed from cadaver data as described in Schneider et al. (1).

Figure 9 shows the force-deflection curves for two impacts to the lower ribcage. Again, the two curves are from tests conducted before and after the sled test series. In both cases, the TAD-50M responses fall within the preliminary corridor and agree with each other. The "point" of maximum force that lies slightly above the corridor was determined to be due to the impactor face contacting the abdominal support bracket, as evidenced in the high-speed films by the impactor "pushing" the dummy rearward.

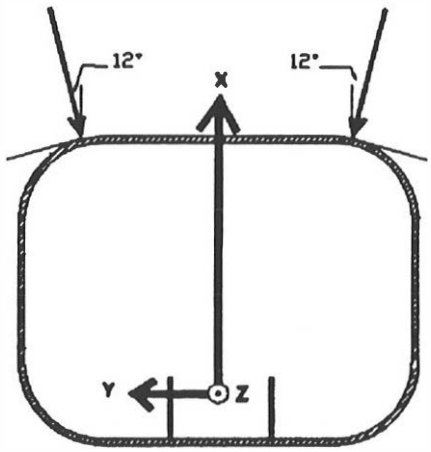

Figure 8. Lower Ribcage Axis of Compression for TAD Pendulum Impacts

Sled Tests

Sled tests were performed with both the TAD-50M and Hybrid III. The 48-kph sled pulse was based on an average of twenty-five 48-kph barrier crash test pulses using mid-size cars. Tests were therefore actually performed at a velocity of 54-kph (which includes a 6-kph rebound velocity) and a peak acceleration of 23 Gs. In a similar manner, the 56-kph sled test pulse was based on an average of twenty-five 56-kph barrier crash test pulses. Tests were therefore performed with a change of veloeity of 63 kph (which includes rebound velocity) and 25 Gs maximum acceleration. Table 1 provides a complete list of the tests conducted.

A listing of the transducers used in both the TAD and Hybrid III sled tests is given in Table 2. In addition to the standard transducers, chest bands (6) were placed externally around the thorax of each dummy at the levels of the upper and lower ribcage. The results obtained from the chest bands will not be presented in this paper, but will be addressed in future analyses.

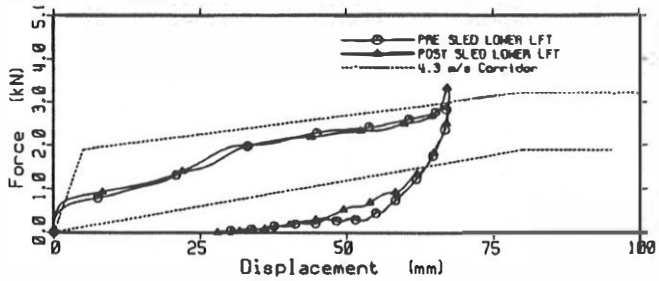

Figure 9. TAD Pre and Post Sled Test Pendulum Impacts - 4.3 m/s Lower Ribcage

In addition to the standard Hybrid III chest potentiometer, a series of eight stringpots was incorporated into the Hybrid III chest using a configuration described by Pritz (7). As illustrated in Figure 10, four of the string pots are connected directly between the sternum and spine box at the first and sixth ribs and the other four are "crossover" string pots. A computer program calculates both the X- and Y-displacements of the rib attachment points.

TABLE 2. TAD-50M and Hybrid III Sled Test Instrumentation

Instrumentation Filter	TAD-50M Torso	Hybrid III	SAE Class
4 DGSP Thoracic Deflection Assemblies	X		180
8 Thoracic Deflection Stringpots		X	180
2 - 24 Gage Chest Bands	X	X	180
Triaxial Head Accelerometers	X	X	1000
Triaxial Pelvic Accelerometers	X	X	1000
Triaxial Chest Accelerometers	X	X	180
3 MHD Angular Velocity Sensors	X		1000
Femur Load Cells	X		600
Triaxial Neck Load Cell	X		1000
Standard Chest Potentiometer		X	180
Seat Belt Load Cells	X	X	60

Sled Test Results and Discussion

For sled tests, direct comparisons of chest deflection patterns between TAD and Hybrid III are not possible due to differences in chest deflection measurement locations (Figure 11), ribcage geometry, and the fact that TAD includes Z-deflection measurement capability. This paper will therefore focus on the performance of the TAD thorax in various restraint environments, including air bag/lap belt, three-point belt, three-point belt/air bag, and two-point belt/knee bolster configurations, rather than attempt detailed comparison to the Hybrid III. Test results for both dummies are summarized in Table 3. All TAD deflections are calculated relative to the spinal X, Y, and Z-axes as shown previously in Figure 4. Deflections quoted in the table are peak values, and are not in general coincident in time.

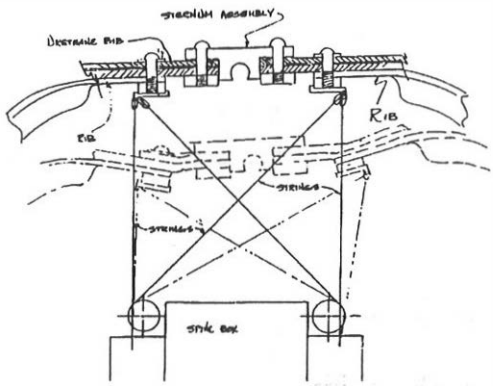

Figure 10. Horizontal Cross Section of Hybrid III Thorax

In many cases, results from the frangible abdominal inserts used in TAD sled tests proved difficult to interpret due to dents and crushing of the insert by lower ribcage intrusion. This interference made intrusion of the seat belt into the abdomen difficult to detect.

48 kph TAD Tests

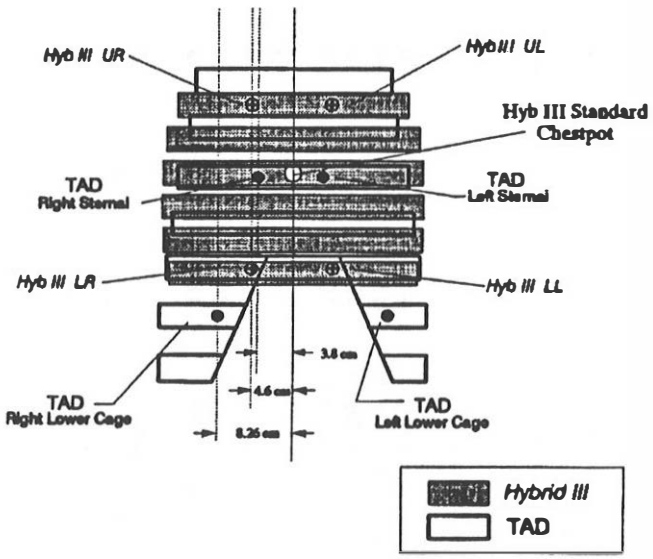

Figure 11. TAD and Hybrid III Deflection Sensor Locations

Figures 12 and 13 show X-Y plane plots (i.e., views from the top) for the sternal and lower ribcage deflections for a test with lap belt and air bag restraint systems (Test 478). These plots were created using the deflection-time histories of the right- and left-sternal (Figure 12) and right- and left-lower (Figure 13) ribcage sensors and represent the motion of the anterior sensor attachment points in the X-Y plane (as defined in Figure 4) as viewed from the top. Dashed-lines connecting the left and right sensor locations at various time intervals are provided to illustrate time sequence, but do not represent the shape of the sternum between sensor attachment locations. The horizontal axis represents the initial X-position of each sensor attachment point. Movement of the sensor above this axis represents an expansion of the ribcage, while deflection below this line corresponds to chest compression. Vertical lines through the left and right sensors

TABLE 3. TAD and Hybrid III Sled Test Maximum Measurements

	TAD 48 kph Tests							TAD 56 kph Tests				Hybrid III 48 kph Tests	
Test Number	**472**	**473**	**474**	**475**	**476**	**477**	**478**	**479**	**480**	**481**		**485**	**486**
Configuration	**Driver 3 Point Belt With Air Bag**	**Driver 3 Point Belt With Air Bag**	**Driver Air Bag**	**Driver 3 Point Belt**	**Driver 3 Point Belt**	**Passenger 2 Point Belt Knee Bolster**	**Driver Lap Belt /Air Bag**	**Driver 3 Point Belt With Air Bag**	**Driver Lap Belt /Air Bag**	**Driver 3 Point Belt**		**Driver Lap Belt /Air Bag**	**Driver 3 Point Belt**
HIC	639	646	373	1413	1273	994	400	762	—	1745		392	1169
Max Head Result (G)	66	64	56	166	157	92	62	76	—	205		59	209
Max Chest Result (G)	51	53	71	56	51	52	48	61	62	59		46	50
Lap Belt Inboard Force (N)	—	----	—	—	—	—	7212	----	8022	—		8926	----
Lap Belt Outboard Force (N)	6086	7251	—	8691	7972	----	7751	8441	8440	8546		9451	9346
Shoulder Belt Inboard Force (N)	—	—	—	—	—	11040	----	----	----	----		----	----
Shoulder Belt Outboard Force (N)	8002	8232	—	8902	8659	7234	—	8598	—	9428		—	8803
Chest Pot (mm)	----	—	—	—	----	—	—	—	----	----		40	43
Maximum Deflections													
Right Sternum X	-49	-51	-56	-48	-48	-24	-45	-49	-31	-51	UR Defl X (mm)	-47	-50
Left Sternum X	-15	-18	-58	-15	-14	-69	-34	-14	-25	-15	UL Defl X (mm)	-39	-30
Right Lower Cage X	-33	-39	16	-37	-38	13	9	-35	13	-37	LR Defl X (mm)	-29	-45
Left Lower Cage X	10	12	-6	13	14	-57	11	14	12	13	LL Defl X (mm)	-19	-13
Right Sternum Y	23	28	-4	32	32	-25	7	33	-5	35	UR Defl Y (mm)	-3	-8
Left Sternum Y	17	21	6	25	20	-33	9	22	4	21	UL Defl Y (mm)	9	11
Right Lower Cage Y	34	35	11	37	36	-14	7	39	5	41	LR Defl Y (mm)	-3	6
Left Lower Cage Y	11	12	-8	11	10	-67	-9	14	-9	12	LL Defl Y (mm)	9	-4
Right Sternum Z	-6	-17	-13	-18	-15	-30	30	-17	22	-20	UR Defl Z (mm)	----	----
Left Sternum Z	-13	-10	-13	10	13	-31	28	13	23	13	UL Defl Z (mm)	----	----
Right Lower Cage Z	12	10	13	17	20	-19	29	17	36	16	LR Defl Z (mm)	----	----
Left Lower Cage Z	8	12	-9	12	17	-14	24	20	37	14	LL Defl Z (mm)	----	----

represent the initial Y-position of each sensor attachment point. Movement to the left or right of the vertical corresponds to leftward or rightward movement respectively. Figure 12 illustrates an inward (X) uniform movement of the sternum with both the right and left sternal points moving slightly towards the left. The lower ribcage moves slightly outward (Figure 13) since the paths traced by the two lower sensors are above the horizontal axis.

These results are further illustrated in the deflection-time history plots of Figures 14 through 16 which show the X-, Y-, and Z-deflections, respectively for the four measurement sites. These plots follow the sign conventions noted in Figure 4. At the level of midsternum, the deflections are inward and similar on both sides while at the lower ribcage the deflections are outward. The flat portion of the traces for the lower ribcage sensors beginning at approximately 60 msec may indicate that the lower sensors have reached their expansion stroke limit, which is approximately 10 to 15 mm. The Y-deflections shown in Figure 15 for this test are seen to be small (less than 9 mm), while the Z-deflections (Figure 16) indicate the anterior ribcage exhibits rather uniform upward z-deflection of about 24-30 mm until approximately 70 msec, at which time the sternal region begins to move downward while the lower ribcage remains pushed up. This may result from the introduction into the TAD design of the mid-thoracic articulation since the upper and lower ribs are able to move separately rather than being constrained to act as a unit.

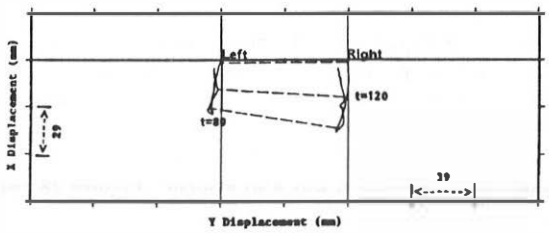

Figure 12. TAD Test 478 Air Bag/Lap Belt - Sternal Sensors (Top View)

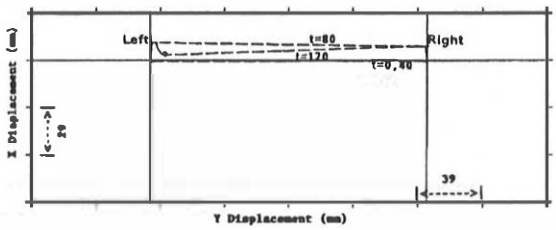

Figure 13. TAD Test 478 Air Bag/Lap Belt - Lower Sensors (Top View)

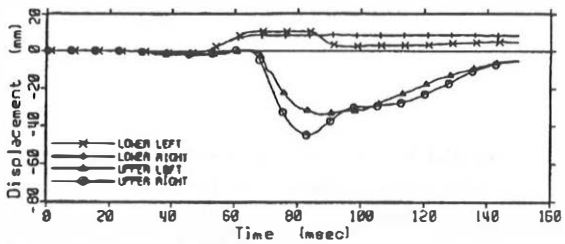

Figure 14. TAD Test 478 Lap Belt/Air Bag - X Deflection

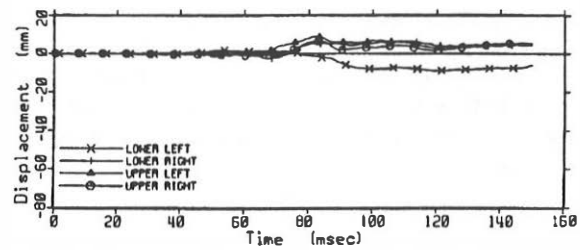

Figure 15. TAD Test 478 Lap Belt/Air Bag - Y Deflection

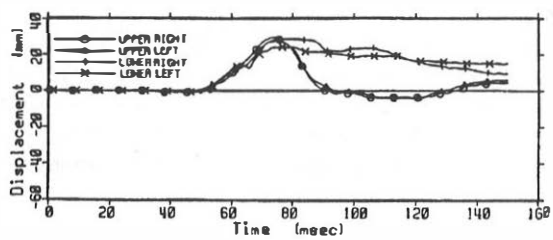

Figure 16. TAD Test 478 Lap Belt/Air Bag - Z Deflection

Figures 17 and 18 show the X-Y plane plots for the sternal and lower ribcage for test 475, a test with three-point-belt restraint only. Both the upper and lower ribs are shown to compress more on the right side than on the left. This result is consistent with the fact that the shoulder belt path lies closer to the right sternal deflection assembly attachment. This result also illustrates that the right and left sternum are largely decoupled in the TAD design.

Figures 19 through 21 show the time histories for this test. Confirming the X-Y plane plots, the X-deflections shown in Figure 19 indicate that the majority of compression occurs on the right side. At the lower ribcage locations, the right-side X-deflection (under the belt path) peaked at 38 mm of inward compression, while the left side exhibited expansion of 14 mm. The Y-deflection plot reveals that the thorax was pulled to the left by the shoulder belt. This phenomenon is most prevalent on the lower right side of the thorax where peak Y-deflection was 37 mm, compared to a peak Y-deflection of 11 mm at the left lower ribcage. Thus, the right lower ribcage is seen to move with considerable independence of the left lower ribcage.

The Z-deflection plot shown in Figure 21 reveals that the right side deflection sensors moved downward initially. At approximately 70 ms, both lower sensors move upward while both upper sensors begin to move downward.

Figures 22 through 26 show the X-Y plane plots and deflection-time histories for test 472, a three-point belt/air bag test. When compared to the three-point belt test (475) described above, the responses appear very similar. Since this test includes an air bag along with the three-point belt restraint, one would anticipate a decrease in peak chest compression due to the presence of the air bag. This is not the case, however.

The shoulder-belt force-time histories for both tests are shown in Figure 27. This plot reveals that the belt forces are identical until approximately 70 ms. At that point, the air bag/three-point belt configuration shows only a slight decrease (approximately 10%) in the shoulder belt force, suggesting that the belt/bag configuration was not optimized. In general, the three-point belt system appears to dominate overall restraint performance in tests 472/473. Under these conditions, the TAD-50M thorax detected little benefit from addition of the nonoptimal air bag and responded accordingly.

In the two-point-belt/knee-bolster test (test 477), a unique deflection pattern was also evident. Figures 28 and 29 show the X-Y plane plots for the sternal and lower ribcage, respectively. The maximum sternal deflection occurred on the left, which is consistent with the fact that the shoulder belt lay to the left of the midsternum since the test was run in the passenger position. The peak compression of 69 mm was the largest X-deflection value recorded in the test series at the sternum and, at the lower-left ribcage, which is under the belt path for this test, the X-deflection of 57-mm compression was also the largest recorded in the test series at this location. The time histories for the two-point-belt test (Figures 30 through 32) further illustrate the inward (X) deflection of the chest, especially on the left side. The Y-deflection time histories reveal significant lateral motion (up to 67 mm) of the ribcage towards the right side. The Z-deflection plot (Figure 32) indicates that the left side of the ribcage is pulled downward while the right side is pushed up slightly and then downward. This test exhibits peak sternal Z-deflections that are approximately twice those obtained in the three-point-belt tests (475/476).

48 kph HYBRID III Tests

Figure 33 shows the X-Y plane plot from test 485, an air bag/lap-belt test of Hybrid III, where the deflections shown are calculated from the triangulated string potentiometers previously described. As shown, the Hybrid III chest reveals a sternal deflection pattern similar to that of the TAD in the same restraint (Figure 12). The chest compresses rather uniformly in the X-direction with little Y-displacement. At the lower ribcage, however, the TAD exhibits expansion (Figure 13) while the Hybrid III experiences compression (Figure 34) due to the stiffer coupling in the Hybrid III and major differences in ribcage geometries between the TAD and Hybrid III designs.

X-Y plots for the three-point belt test of Hybrid III (test 486) are shown in Figures 35 and 36 and indicate the same type of deflection pattern as seen in the TAD (Figures 17 and 18). At the sternum, the thorax compresses more on the right than on the left as one would expect in this configuration. However, the TAD exhibits a larger difference in the inward sternal deflections between the left and right side than does the Hybrid III. This is illustrated by the fact that the angle subtended by a line connecting the left and right measurement points and the horizontal is approximately 25 degrees in the TAD sternal deflection (Figure 17) and only about 15 degrees in the Hybrid III at the upper sensors (Figure 35). In addition, the Hybrid III exhibits smaller Y-deflections than does the TAD, at both the sternum and lower ribcage. Also, the Hybrid III experiences only compression at the lower ribcage (Figure 36), while the TAD demonstrates compression on the right and expansion on the left at the lower ribcage (Figure 18).

56 kph TAD Tests

Results from test 481, a three-point belt test of the TAD, can be compared with test 475 of the TAD conducted at the lower velocity. As seen from Table 3, somewhat higher chest Gs and higher head resultant acceleration upon contact with the steering assembly are noted, but the differences in thorax X, Y and Z peak deflections are small. However, it may be noted that measured lap belt and shoulder belt peak loads are only slightly higher (5-7%) than those measured in test 475.

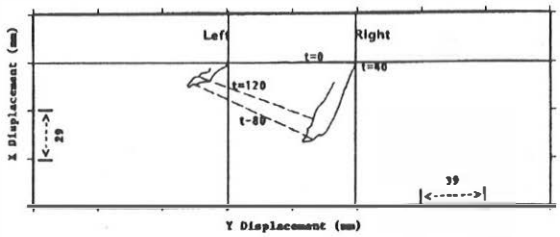

Figure 17. TAD Test 475 Three-Point Belt - Sternal Sensors (Top View)

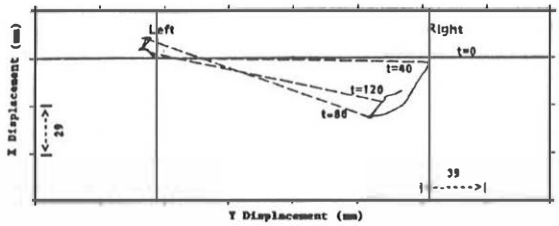

Figure 18. TAD Test 475 Three-Point Belt - Lower Sensors (Top View)

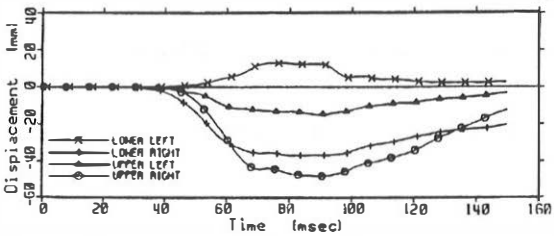

Figure 19. TAD Test 475 Three-Point Belt - X Deflection

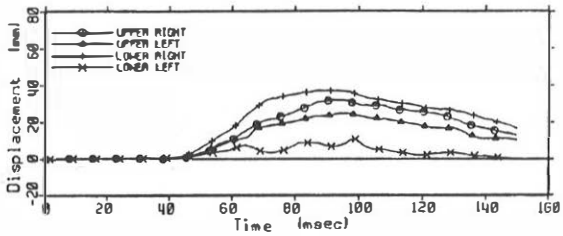

Figure 20. TAD Test 475 Three-Point Belt - Y Deflection

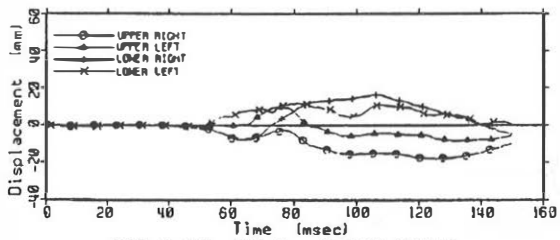

Figure 21. TAD Test 475 Three-Point Belt - Z Deflection

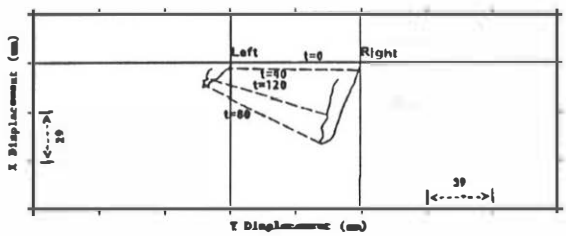

Figure 22. TAD Test 472 Three-Point Belt/Air Bag - Sternal Sensors (Top View)

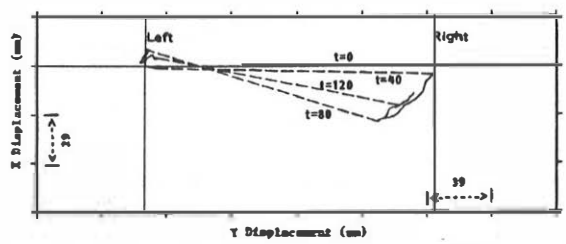

Figure 23. TAD Test 472 Three-Point Belt/Air Bag - Lower Sensors (Top View)

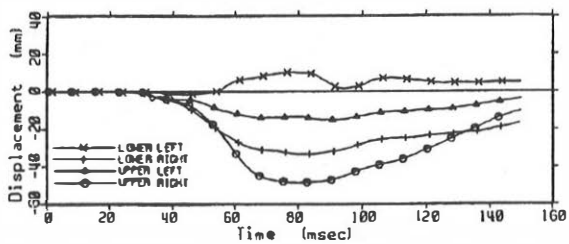

Figure 24. TAD Test 472 Three-Point Belt/Air Bag - X Deflection

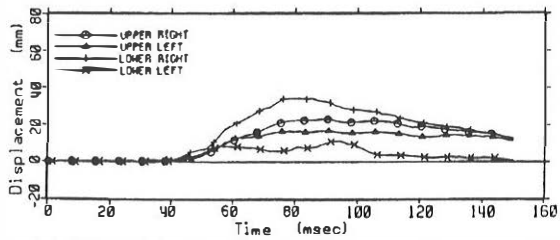

Figure 25. TAD Test 472 Three-Point Belt/Air Bag - Y Deflection

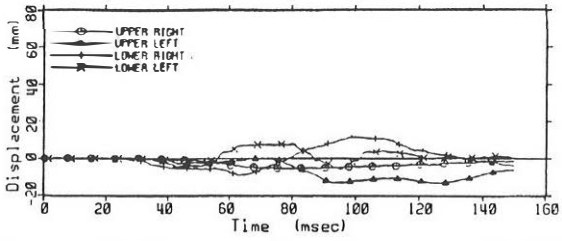

Figure 26. TAD Test 472 Three-Point Belt/Air Bag - Z Deflection

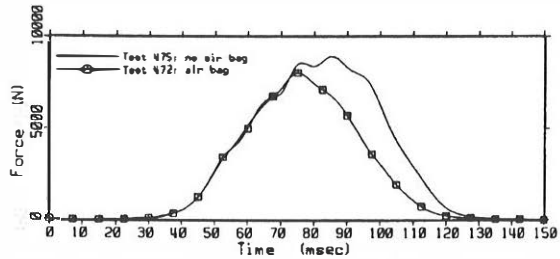

Figure 27. TAD Three-Point Belt Shoulder Belt Force With and Without Air Bag

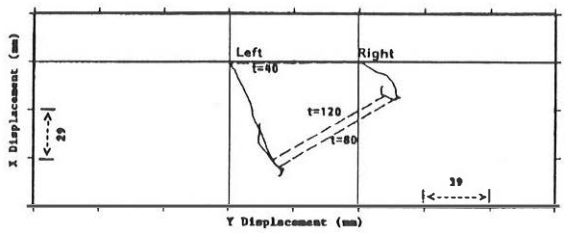

Figure 28. TAD Test 477 Two-Point Belt/Knee Bolster - Sternal Sensors (Top View)

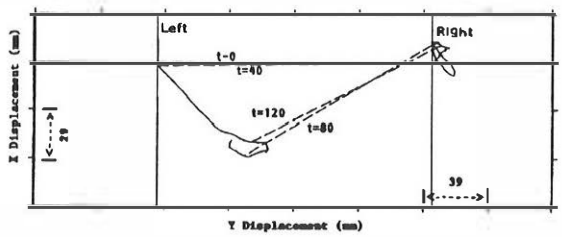

Figure 29. TAD Test 477 Two-Point Belt/Knee Bolster - Lower Sensors (Top View)

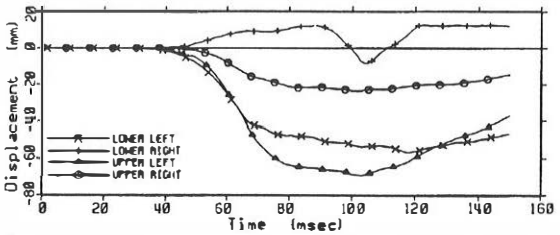

Figure 30. TAD Test 477 Two-Point Belt/Knee Bolster - X Deflection

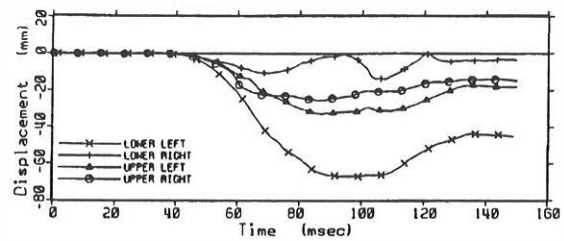

Figure 31. TAD Test 477 Two-Point Belt/Knee Bolster - Y Deflection

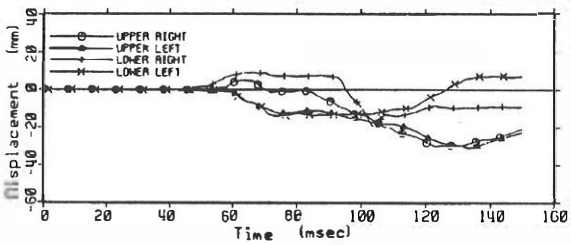

Figure 32. TAD Test 477 Two-Point Belt/Knee Bolster - Z Deflection

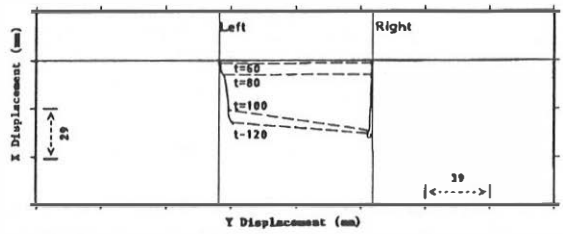

Figure 33. Hybrid III Test 485 Air Bag/Lap Belt - Upper Sensors (Top View)

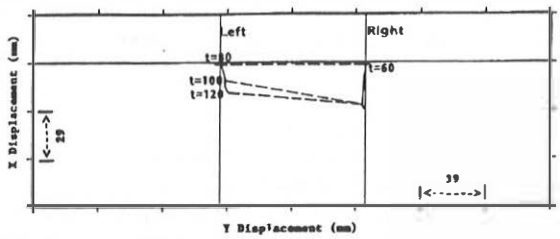

Figure 34. Hybrid III Test 485 Air Bag/Lap Belt - Lower Sensors (Top View)

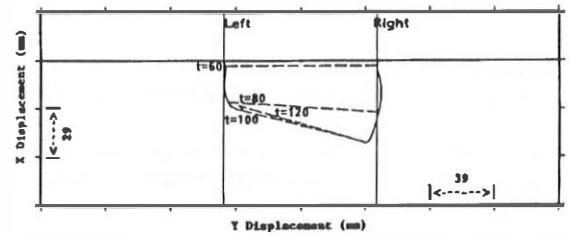

Figure 35. Hybrid III Test 486 Three-Point Belt - Upper Sensors (Top View)

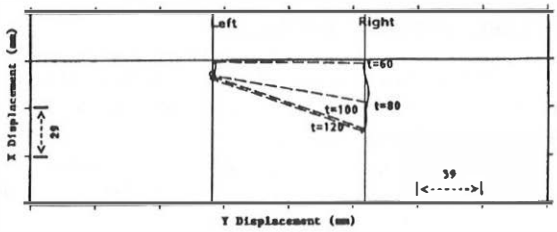

Figure 36. Hybrid III Test 486 Three-Point Belt - Lower Sensors (Top View)

Similar differences are noted for three-point-belt/air bag tests at 48 kph (tests 472/473) and the same test configuration (test 479) at 56 kph. The response of the dummy to the higher velocity was not significantly different from that at the lower velocity.

A comparison of the test pulses from the 48-kph and 56-kph tests reveals why the results of the same test configurations did not differ significantly for the two different velocities. Figure 37 shows a comparison of sled velocity-time histories for the two tests and reveals the velocities to be nearly identical up to 80 ms. The differences in impact severity experienced by the TAD were small up to the time of maximum deflection, thereby explaining why the results for the 48-kph and 56-kph tests do not differ significantly. Further evidence for these results can be seen in the shoulder-belt force-time plots for tests 475 and 481 of Figure 38. The peak belt force is only slightly higher in the 56-kph test when compared to the 48-kph test.

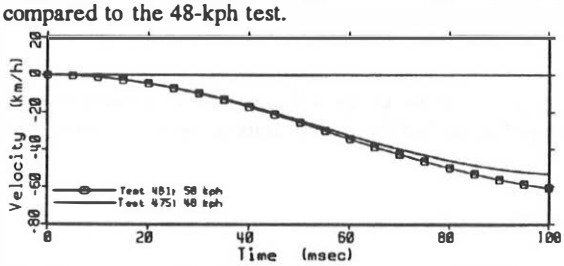

Figure 37. TAD Three-Point Belt Sled Velocities for 48 and 56 kph Tests

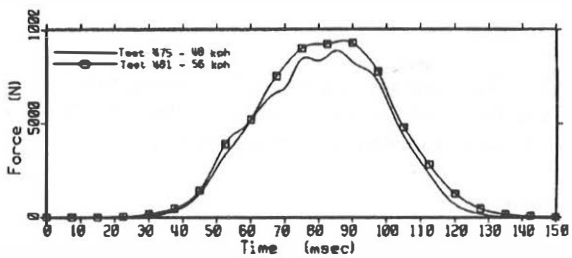

Figure 38. TAD Three-Point Belt Shoulder Forces for 48 and 56 kph Tests

Finally, test 480, a lap-belt/air bag test of the TAD, is interesting because a failure in the steering column attachment to the sled buck resulted in steering column stroke that did not occur in the other tests. Under this condition, it is noted that sternal X-deflections were significantly reduced (Table 3). Consistent with results of test 478, test 480 demonstrated very small Y-deflections, typical of air bag loading in this test series, and uniform upward Z-deflections of the anterior ribcage.

Conclusions

Based on the results of this test series, the following conclusions can be drawn with regard to the performance of the TAD-50M prototype thorax system:

1. For sternal impacts at 6.7 m/s, the response falls within the recommended corridor. At 4.3 m/s sternal impacts, the computed peak inward deflection falls short of the desired corridor.

2. The impact response at the lower ribcage for 4.3 m/s impacts agrees well with the preliminary Neathery force-deflection corridor described in Schneider et al. (1).

3. The TAD deflection instrumentation and accompanying software proved functional and accurate to within 2 mm.

4. The TAD thorax system appears to discriminate the degree of concentration of restraint loading, the degree of symmetry of restraint loading, and the intensity of local loading to the sternal region and lower ribcage.

5. The TAD has proven to be quite durable in extended pendulum and sled testing, and suffered no significant structural or functional failures.

6. When compared to the response of the Hybrid III tested in the same configuration, the TAD thorax responds in a more compliant, decoupled manner.

7. The lower ribcage of the TAD proved necessary to capture significant two-point belt system response features.

8. The TAD thorax exhibits promise as a useful tool to assess the performance of combined belt/air bag restraint systems.

Recommendations for Future Work

1. Consideration should be given to an additional displacement measurement assembly at the sternum between the present deflection sensors in order to appreciate the curvature at the sternum as well as for comparison with the Hybrid III standard deflection potentiometer.

2. Provisions should be considered to increase the expansion travel of the joy sticks, especially at the lower ribcage.

3. Future analysis of additional TAD instrumentation is recommended, such as chest bands and MHD 's, which will provide further information regarding chest deflection and spinal kinematics.

Acknowledgements

The TAD-50M thorax system was developed under contract to the U.S. Department of Transportation, National Highway Traffic Safety Administration (NHTSA) by a team consisting of the University of Michigan Transportation Research Institute, First Technology Safety Systems, Wayne State University, and Oklahoma State University. Significant contributions to the development were also made by General Motors Research Laboratories, the SAE Frontal Impact Dummy Enhancement Task Group, and the NHTSA Biomechanics Division.

This evaluation was performed by the Transportation Research Center, Inc. (TRC) at the Vehicle Research and Test Center (VRTC) under contract to the National Highway Traffic Safety Administration (NHTSA), U.S. Department of Transportation.

The authors wish to acknowledge Kenneth Welty (VRTC), Howard Pritz (VRTC),and Duane Stoltzfus (TRC), for their technical support during this project as well as Susan Weiser (VRTC) and Edward Parmer (TRC) in the preparation of this paper.

Disclaimer

The opinions, findings and conclusions expressed in this paper are those of the authors and not necessarily those of the Transportation Research Center, Inc., the National Highway Traffic Safety Administration, or the University of Michigan Transportation Research Institute.

References

1.Schneider, L.W., Ricci, L.L., Salloum, M.J., Beebe, M.S., Rouhana, S.W., King, A.I., and Neathery, R.F.,"Design and Development of an Advanced ATD Thorax System for Frontal Crash Environments: Final Report Volume 1: Primary Concept Development," U.S. Department of Transportation, National Highway Traffic Safety Administration, in press, 1992.

2. Kroell, C.K., Schneider, D.C., and Nahum, A.M., "Impact Tolerance and Response to the Human Thorax," Proc. 15th Stapp Car Crash Conference, p. 84-134, Society of Automotive Engineers, Warrendale, PA, 1971.

3. Kroell, C.K., Schneider, D.C., and Nahum, A.M., "Impact Tolerance and Response to the Human Thorax II," Proc. 18th Stapp Car Crash Conference, p. 383-457, Society of Automotive Engineers, Warrendale, PA, 1974.

4. Neathery, R.F., "Analysis of Chest Impact Response Data and Scaled Performance Recommendations," Proc. 18th Stapp Car Crash Conference, 1974.

5. Schneider, L.W., King, A.I., and Beebe, M.S., "Design Requirements and Specifications: Thorax - Abdomen Development Task. Interim Report. Trauma Assessment Device Development Program," Report DOT HS 807 511, U.S. Department of Transportation, National Highway Traffic Safety Administration, 1989.

6. Hagedorn, A.V., Eppinger, R.H., Morgan, R.M., Pritz, H.B., and Khaewpong, N., "Application of a Deformation Measurement System to Biomechanical Systems," Proc. IRCOBI Conference, 1991.

7. Pritz, H.B., "Development and Evaluation of Hybrid III Multi-Point Thoracic Deflection Measurement Sensors," Draft Report VRTC-87-0076, U.S. Department of Transportation, National Highway Traffic Safety Administration, 1990.